Cah. Biol. Mar. (1998) 39 : 169-184

Vulcanoctopus hydrothermalis gen. et sp. nov. (Mollusca, Cephalopoda): an octopod from a deep-sea hydrothermal vent site

Angel F. GONZÁLEZ[1]*, Angel GUERRA[1], Santiago PASCUAL[2] and Patrick BRIAND[3]
1 Instituto de Investigaciones Marinas (C.S.I.C.), Eduardo Cabello 6, E-36208 Vigo, Spain
2 Laboratorio de Parasitología, Facultad de Ciencias del Mar, Universidad de Vigo, Ap. 874. E-36200 Vigo, Spain
3 IFREMER, Centre de Brest, DRO/EP/CENTOB, BP 70, 29280-Plouzané, France.
** Corresponding author*
Fax: (34) 9 86 29 27 62; e-mail: afg@iim.csic.es

Abstract: We describe two specimens of an octopod from a hydrothermal vent of the East Pacific Rise (13°N, 2640 m) collected during the French cruise HOT 96 (CNRS/IFREMER). They are two males, one immature and one mature. The diagnosis of this new genus is as follows: benthic animals with a muscular and semi-translucent body; lack of any type of chromatic elements in the skin; eye with no trace of an iris; presence of a large white body covering the eye-ball, the optic nerves and the optic lobe; digestive gland multilobulate; presence of a black bulb, here called dark swelling, in proximal third of the intestine; presence of a crop and absence of an ink sac. The new species *Vulcanoctopus hydrothermalis* is a small benthic animal up to 35 mm mantle length. The posterior part of the mantle is mitre-like. Arms 2.5-4 times the length of the mantle. Right arm III hectocotylized. Ligula short (9.5 % of the hectocotylized arm), lance-shaped and without transverse ridges. Calamus short (17.9% of the ligula length). In adult males enlarged suckers absent, and the diameter of the largest sucker is about 6% of the mantle length. Depth of the largest sector of the web about 4.8% of the longest arm. Gills with eight lamellae per demibranch. The possibility of raising a new sub-family (Vulcanoctopodinae) of Octopodidae, the ecology and adaptations of these vent animal are discussed.

Résumé : Vulcanoctopus hydrothermalis, *gen. et sp. nov. (Mollusca, Cephalopoda) : un octopode des sources hydrothermales profondes.* Nous décrivons ici deux spécimens d'un octopode des sources hydrothermales de la ride du Pacifique oriental (13°N, 2640 m) récoltés pendant la campagne française HOT 96 (CNRS/IFREMER). Ces deux individus sont des mâles, l'un immature et l'autre mature. La diagnose du genre *Vulcanoctopus* est la suivante : animaux benthiques avec un corps musculeux semi-translucide ; absence d'éléments chromatiques dans la peau ; yeux sans iris ; corps blanc très développé recouvrant le globe oculaire, les nerfs optiques et le lobe optique ; glande digestive multilobée ; absence de poche à encre. La nouvelle espèce *V. hydrothermalis* est une petite espèce benthique dont le manteau ne dépasse pas 35 mm de longueur. La partie postérieure du manteau est en forme de mître. Les bras ont 2,5 à 4 fois la longueur du manteau. Le troisième bras droit (III) est le bras hectocotyle, sa partie terminale (ligula) est courte (9,5 % de la longueur du bras), élancée et sans stries transversales. Calamus court (17,9 % de la longueur de la ligula). Chez le mâle adulte les ventouses hypertophiées sont absentes, leur diamètre moyen étant d'environ 6 % de la longueur du manteau. La profondeur du plus grand secteur du voile est d'environ 4,8 % de la longueur du plus long bras. Huit lamelles par demi-branchie. La possibilité de la création d'une nouvelle sous-famille (Vulcanoctopodinae) chez les Octopodidae, l'écologie et les adaptations de cet organisme hydrothermal sont discutées.

Keywords : *Vulcanoctopus hydrothermalis*, Octopodidae, cephalopod, hydrothermal vent, East Pacific Rise.

Reçu le 5 janvier 1998; accepté après révision le 1er juillet 1998.
Received 5 January 1998; accepted in revised form 1st July 1998.

Introduction

Historically, little research has been carried out on cephalopods from deep-sea hydrothermal vents. To date, the few cephalopods collected in several expeditions using deep-diving submersibles at the East Pacific Rise (Desbruyères et al., 1982; Fustec, 1985; Desbruyères & Segonzac, 1997) have not been studied in detail. The only information existing about cephalopods from hydrothermal vents is the description of two octopods engaged in a copulatory behaviour documented by a videotape record (Lutz & Voight, 1994) and the description of some specimens of *Graneledone* spp. and *Benthoctopus* spp. from the Middle Valley and Juan de Fuca Ridge in the Northeast Pacific (Lutz & Voight, 1997).

The existence of hydrothermal vents was first suspected at the East Pacific Rise in 1976 on the Galapagos Rift (Londsdale, 1977). Black smokers are chimneys up to 10 m high, where hot water gushes out of the vents in the sea-bed at temperatures of 265°C forming a dense plume of black 'smoke' made up of minute particles of metal sulphides (Campbell et al., 1988). To collect samples or to undertake in situ studies at deep-sea habitats is extremely difficult, in such a hostile environment. The mobility of cephalopods represents an additional difficulty. However, a long series of deep-sea submersible-based research expeditions conducted by several nations has resulted in detailed description of the community organization and various aspects of the biology of some prominent inhabitants of the vent fauna (Chevaldonné, 1997). In the case of octopods, the greater part of the material obtained represents the cirrate octopods, whose behaviour has been described from videotape records (Villanueva et al., 1997), while few have been captured by submersibles (Guerra et al., in press).

Deep-sea octopods have colonized practically all the habitats throughout the oceans from beneath the ice fields of the Arctic and the Antarctic to the deep ocean trenches below 7000m (Voss, 1988). The significance of the marked gradients of pressure and temperature for deep-sea octopods has not yet been studied whereas they may play an important role in speciation (Clarke & Trueman, 1988). Hydrothermal vent characteristics, where a surprising associated fauna has been described (see Gage & Tyler, 1991; Desbruyères & Segonzac, 1997), represent a challenge to the documented adaptive capacity of cephalopods. It is known that this peculiar ecosystem is inhabited by octopods, but little is known about adaptations of these animals to survive in this extreme environment.

Two specimens of a benthic octopodid collected close to a deep-sea hydrothermal vent in the East Pacific Rise are described in the present study. The functional morphology of some structures found in these specimens is discussed.

Material and methods

Two octopods were caught not far from a high temperature hydrothermal vent (black smoker) with the aid of a vacuum installed in the manned submersible *Nautile* during HOT 96, a biological programme of the French Research Vessel *Nadir* organized by CNRS, Paris VI and IFREMER-Brest (chief scientist: F. Gaill). Both octopods were collected as part of biological sampling of species inhabiting the East Pacific Rise (Fig. 1). The area studied (12°48.43'N-103°56.41'W; 2647 m depth) is situated north to the site commonly known as Genesis that was first observed in March 1984. The temperature in Genesis ranges from 1-1.6°C in the surrounding sea water, 1.6-10°C around the *Riftia pachyptila* plume, 7-91°C close to the populations of Polychaeta Alvinellidae, up to 262-269°C in the fluid of the vent (Sarradin et al., 1998).

The holotype (Fig. 2) is a specimen caught in dive PL 1067, a fully mature male of 34.7 mm dorsal mantle length (ML, Table 1), collected on 19/02/96, two meters from the East wall of the main black smoker of Genesis on a basaltic plateau. The associated fauna that colonizes the chimney is composed of Vestimentifera (tube-worms: *Riftia pachyptila* Jones, 1985 and *Tevnia jerichonana* Jones, 1985, Polychaeta Alvinellidae: *Alvinella* spp., turrid gastropods:

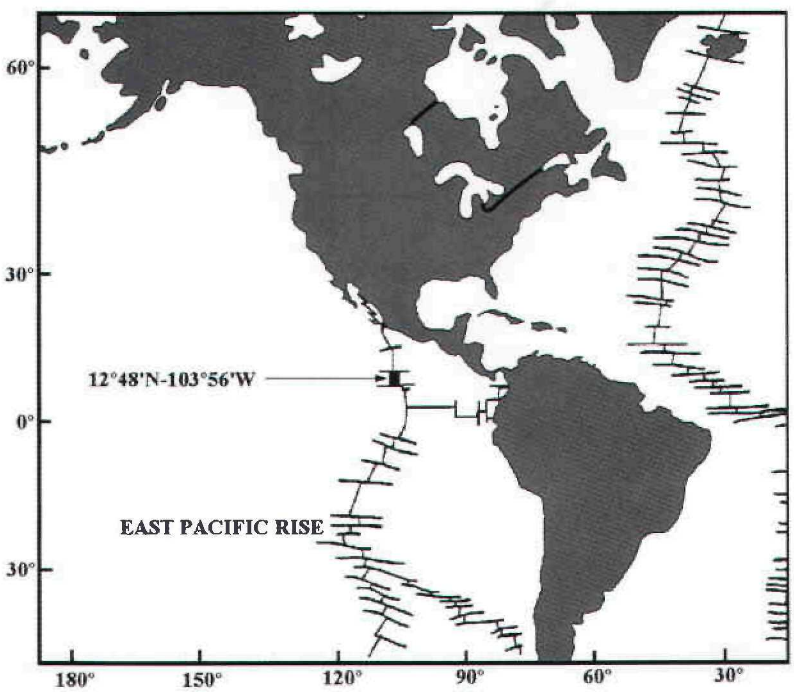

Figure 1. Map showing the locality where *Vulcanoctopus hydrothermalis* gen. et sp. nov. has been collected (filled square).

Figure 1. Carte montrant l'emplacement du lieu de récolte de *Vulcanoctopus hydrothermalis* gen. et sp. nov. (carré noir).

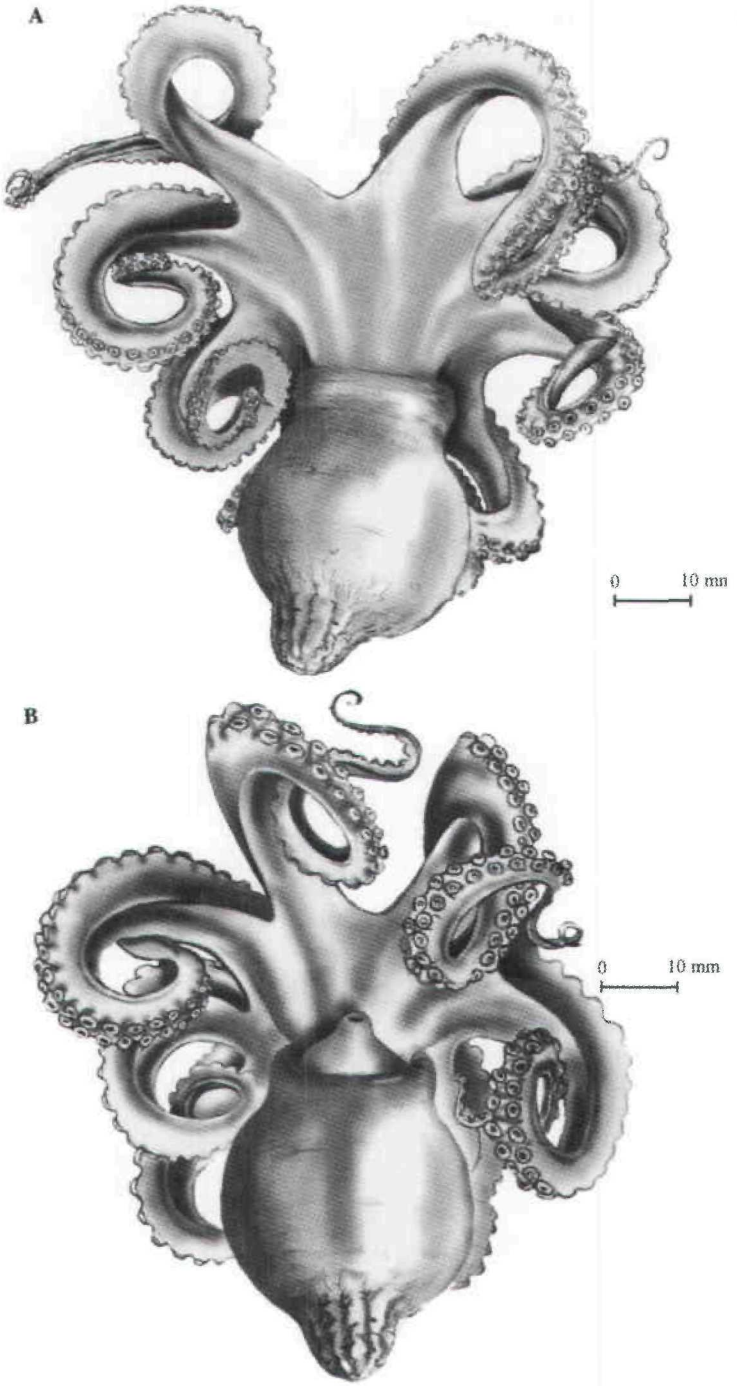

Figure 2. Dorsal (**A**) and ventral (**B**) view of the holotype.
Figure 2. Vue dorsale (**A**) et ventrale (**B**) de l'holotype.

Phymorhynchus spp., the caridean shrimp: *Alvinocaris lusca* Williams & Chace, 1982, the brachyuran crabs: *Bythograea thermydron* Williams, 1980, the galatheid: *Munidopsis subsquamosa* Henderson, 1885, the mussel: *Bathymodiolus thermophilus* Kenk & Wilson, 1985 and a zoarcid fish *Thermarces cerberus* Rosenblatt & Cohen, 1986. These animals were identified from samples taken ashore and with the aid of a video recording (Segonzac, pers. comm.).

The paratype is a specimen collected in dive PL 1061, an immature male of 21.2 mm ML. It was collected at 2647 m depth on 13/02/96, one meter far from the base of a small white smoker (old waning black smoker), north of Genesis. The substrate was a cliff of basaltic rocks covered by oxidate sulphides. The sites of collection of both males were situated 10 metres apart and the associated fauna was similar to that described above (Segonzac, pers. comm.).

The animals were in good condition except for damage to some arms. They were fixed in formaldehyde (4% in sea water) and preserved in 70% alcohol. Only the mature animal was used for histological procedures and analysis of elements.

Definition of counts, measurements and indices follow Roper & Voss (1983), Aldred et al. (1983) and Clarke (1986).

Histological sections were stained by Masson's trichrome method, Wheatley's method or haematoxylin and eosin.

Analysis of elements in several tissues of these animals from deep-sea hydrothermal vents were undertaken for comparison with similar studies carried out in other octopods (Sugiyama et al., 1989; Miramand & Bentley, 1992). Pieces of mantle, lateral vena cava and mesenteric vein of the holotype were removed for metal analysis using flame atomic-absorption spectrophotometry. For these analyses, the tissues were dried at 50°C for several days to constant weight and then ground. Acid digestion of an aliquot (mantle = 0.065 mg; mesenteric vein = 10.036 mg; lateral vena cava = 0.0440 mg) of each sample was performed with nitroperchloric acid mixture. Digestion was undertaken with a Teflon closed-digestor at 250°C. Al, Ba, Ca, Cd, Cu, Fe, K, Li, Mg, Mn, Ni, Pb, Sr and Zn were analysed by flame atomic-absorption spectrophotometry. Calibration was by certified standards.

Taxonomic position

Order Octopoda Leach, 1817
Family Octopodidae d'Orbigny, 1840
Sub-familial status not clear. This issue is analysed in the discussion section.

Vulcanoctopus, González and Guerra, 1998 gen. nov.

Diagnosis
Benthic animals with a muscular consistency and a semi-translucent body, lacking chromatic elements in the skin;

Table 1. Measurements counts and indices of holotype and paratype *Vulcanoctopus hydrothermalis,* gen. et sp. nov.
Tableau 1. Mesures et index de l'holotype et du paratype de *Vulcanoctopus hydrothermalis* gen. et sp. nov.

(AF) *Arm Formula:* Comparative length of arms expressed numerically in decreasing order of arms numbered from dorsal to ventral; (ALI) *Arm Length Index:* oral surface from the lips to the tip of the arm as a percentage of mantle length; (ASC) *Arm Suckers Counts:* number of suckers per row on each arm; (CaLI) Calamus Length Index: length of the calamus measured from the last (distal most) sucker to its distal tip as a percentage of ligula length; (EDI) *Eye Diameter Index:* diameter of eye across bulbus as a percentage of ML; (FFuI) *Free Funnel Index:* the length of the funnel from the anterior funnel opening to the point of dorsal attachment to the head as a percentage of ML; (FuLI) *Funnel Length Index:* from the insertion point into the mantle to the tip as a percentage of ML; (GiLI) *Gill Length Index:* from the proximal filament to tip as a percentage of ML; (HWI) *Head Width Index:* across widest point between the eyes as a percentage of ML; (LCL) *Lower Crest Length:* length from the rostrum to the top of the two lateral walls of the lower beak; (LHL) *Lower Hood Length:* length from the tip of the rostrum to the posterior end of the hood of the lower beak; (LRL) *Lower Rostral Length:* length from the rostrum to the shoulder of the lower beak; (LiLI) *Ligula Length Index:* from distal most sucker to tip of arm as a percentage of hectocotylized arm; (ML) *Mantle Length:* posterior of body to point midway between the eyes; (MWI) *Mantle Width Index:* across widest point as a percentage of ML; (MS) Maturity Stage: Immature or mature; (PAI) *Pallial Aperture Index:* the measurement between the points to the attachment of the mantle to the head along the ventral margin of the mantle as a percentage of ML; (SDI) *Sucker Diameter Index:* the diameter measured across the aperture from outer rim to outer rim as a percentage of mantle length (ML); (SpLI) *Spermatophore Length Index:* total length of the spermatophore as a percentage of ML; (TL) Total Length: from end of longest arm to posterior end of mantle; (UCL) *Upper Crest Length:* length from the rostrum to the top of the two lateral walls of the upper beak; (UHL) *Upper Hood Length:* length from the tip of the rostrum to the posterior end of the hood of the upper beak; (URL) *Upper Rostral Length:* length from the rostrum to the shoulder of the upper beak; (WDI) *Web Depth Index:* measurement of deepest sector of web measured from mouth to midpoint of sector between arms as a percentage of ML. (Web sector A, dorsal to dorsal arm; B, dorsal to dorso-lateral; C, dorso-lateral to ventro-lateral; D, ventro-lateral to ventral; E, ventral to ventral); (WF) *Web Formula:* Comparative depth of each web sector, alphabetically in decreasing order. (I) Immature; (M) mature and (D) damaged.

		Holotype (MNHN 2885)	Paratype (MNHN 2886)
ML		34.7	21.2
MS		M	I
TL		163	103
MWI		83.6	69.8
HWI		55.9	49.5
EDI		19.6	18.9
ALI	L1	372.9	355.2
	L2	D	D
	L3	304.0	345.8
	L4	287.3	285.4
	R1	331.4	D
	R2	D	D
	R3	194.2	D
	R4	304.3	244.3
ASC	L1	80	62
	L2	D	D
	L3	67	65
	L4	68	58
	R1	75	D
	R2	D	D
	R3	40	D
	R4	70	45
SDI		5.7	6.1
SpLI		125.0	I
LiLI		9.0	D
CaLI		17.9	D
WDI	A	12.7	11.9
	B	16.1	14.1
	C	15.0	14.2
	D	14.4	12.5
	E	13.7	9.0
WF		B>C>D>E>A	C>B>D>A>E
PAI		40.9	49.5
GiLI		36.3	42.9
FuLI		27.3	25.0
FFuI		12.9	11.3
URL		1.4	0.6
UCL		5.9	3.8
UHL		1.8	1.5
LRL		0.9	0.5
LCL		4.3	2.7
LHL		1.9	1.2

eyes have no trace of an iris and there is no optic chiasma; presence of a large white body (which covers the eye, the optic nerves and the optic lobe). A crop and a multilobulate digestive gland; an inflated black bulb (here called dark swelling), in proximal third of the intestine; absence of an ink sac.

Etymology

From the Latin, *Vulcanus* (God of fire and smiths), referring to the igneous activity taking place in the area where animals were caught.

Type species: *Vulcanoctopus hydrothermalis* sp. nov. González and Guerra, 1998.

Holotype: male, 34.7 mm ML, HOT 96 East Pacific Rise, North of Genesis, 12°48.43'N-103°56.41'W, depth 2647 m, dive PL1067, coll. P.M. Sarradin, 19 February 1996. Holotype (dissected specimen) deposited in the Muséum National d'Histoire Naturelle Paris, MNHN n° 2885.

Paratype: male, 21.2 mm ML, HOT 96 East Pacific Rise, North of Genesis, 12°48.43'N-103°56.41'W, depth 2647 m, dive PL1061, coll. A.M. Alayse, 13 February 1996. Paratype (dissected specimen) deposited in the Muséum National d'Histoire Naturelle Paris, MNHN n° 2886. The hectocotylus was removed by R. Lutz for genetic studies.

Diagnosis

Small benthic animal up to 35 mm mantle length. The posterior part of the mantle is mitre-like. Arms 2.5-4 times the length of the mantle. Right arm III hectocotylized. Ligula short (9.5% of the hectocotylized arm), lance-shaped and without transverse ridges. Calamus short (17.9% of the ligula length). Adult male has no enlarged suckers, the diameter of the largest sucker being about 6% of the mantle length. Depth of the largest sector of the web about 4.8% of the longest arm. Gills with eight lamellae per demibranch.

Etymology

From the latinized composite term of Greek origin "hydrothermalis", referring to the warm sea water temperature gushing out from the vent.

Description

I. External morphology

Male small, white and muscular (Figs. 3, 5). Mantle wall thin (0.8 mm) and semi-translucent, without chromatic elements in the skin. The mantle is pear-shaped and posteriorly mitre-like and wrinkled after fixation (Fig. 4). Measurements, counts and indices are summarized in Table 1. The head is small (HWI 49.5-55.9), narrower than the mantle width (MWI 69.8-83.6), neck region slightly constricted. The eyes are small (EDI 18.9-19.6) and in fixed specimens, they are entirely covered by the skin of the head except a thinner semi-translucent skin forming a window of 0.2 mm in length, over the eye (Fig. 6). Arms elongated (ALI 244.3-372.9) without cirri. Each of similar size at the base, tapers to a finely attenuated tip (Fig. 7). No enlarged sucker, suckers biserial and small relative to arm length (SDI 5.7-6.1). Right arm III hectocotylized (Fig. 8), shorter (HcAI 194.2) than the opposite arm (ALI 304.0). Ligula lance-shaped (Fig. 18B), its length is 9.5% the length of hectocotylized arm. Copulatory groove shallow without transverse ribs. Spermatophore groove well developed, narrow and smooth. Calamus short (CaLI 7.9). Web symmetric, moderately deep (WDI 9.0-16.1) and the membranes extend as a narrow seam along the dorsal edge to the tip of each arm (Fig. 6). Web formula variable (Table 1). Pallial aperture wide (PAI 40.9-49.5) and U shaped (Fig. 9). Funnel short (FuLI 25-27.3), free portion approximately 1/2 funnel length (Fig. 10). The funnel organ could not be found in these fixed specimens.

II. Mantle cavity

Mantle cavity large, gills situated anteriorly, close to mantle aperture (Fig. 10). Gills moderately long (GiLI 36.3-42.9), whitish, leaflets thick and fleshy, with 8 lamellae per demibranch. No trace of an ink sac. Terminal organ and anus open at the base of the funnel. Branchial hearts, branchial heart appendages, renal appendages and renal sacs well developed.

III. Digestive tract

The alimentary system is shown Fig. 11 A. The buccal cavity, surrounded by the buccal mass provided with two octopus-like beaks (Figs. 11 D-G) and a radula, leads posteriorly into the oesophagus. The radula has 7 teeth and two marginal plates in each transverse row (Fig. 12). Rachidian tooth has one lateral cusp on each side of a large medial cone. Lateral cusps in asymmetrical seriation migrating from lateral to medial portion over 5 rows (B5 type). First lateral tooth small with a lateral cusp. Second lateral tooth with curved base and two cusps on each margin. Third lateral tooth long and dagger-like.

Lying at the back of the buccal mass and wrapped around it are the paired anterior salivary glands.

The oesophagus expands into a well developed crop and continues to the stomach. The paired posterior salivary glands are large and have a butterfly wing-like shape, their own ducts going to the buccal mass.

The caecum is a little smaller than the stomach and does not form a spiral. The stomach and caecum lie ventrally on the multi-lobulate digestive gland. This gland is peculiar and comprises eight lobes, maroonish in colour, with a whitish ventral pancreatic area with a pair of ducts that open into the caecum (Figs. 11 B, C). The intestine is wider than the oesophagus with a black bulb, here called dark swelling, in its proximal third. This structure has not previously been found in a cephalopod. The rectum ends in an anus devoid of anal flaps.

Some unidentified cuticular remains of white crustaceans, probably belonging to galatheids, were found in the stomach of the holotype.

A transverse histological section of the posterior salivary glands shows the gland to be composed of secretory units (Fig. 13) and a single branched secretory duct. Serous and mucous cells are present in the secretory tubules. Secretory ducts are lined by specialized epithelial cells that are surrounded by connective tissue.

The dark swelling has a peripheral wall composed of connective tissue, below which is an outer layer of circular and an inner layer of longitudinal muscular fibres (Fig. 16). The inner wall (submucosa) is longitudinally folded. The epithelium is high and cylindrical. Excretory substances are present in the lumen, but are absent from the intestinal lumen (Fig. 17), on either side of the dark swelling.

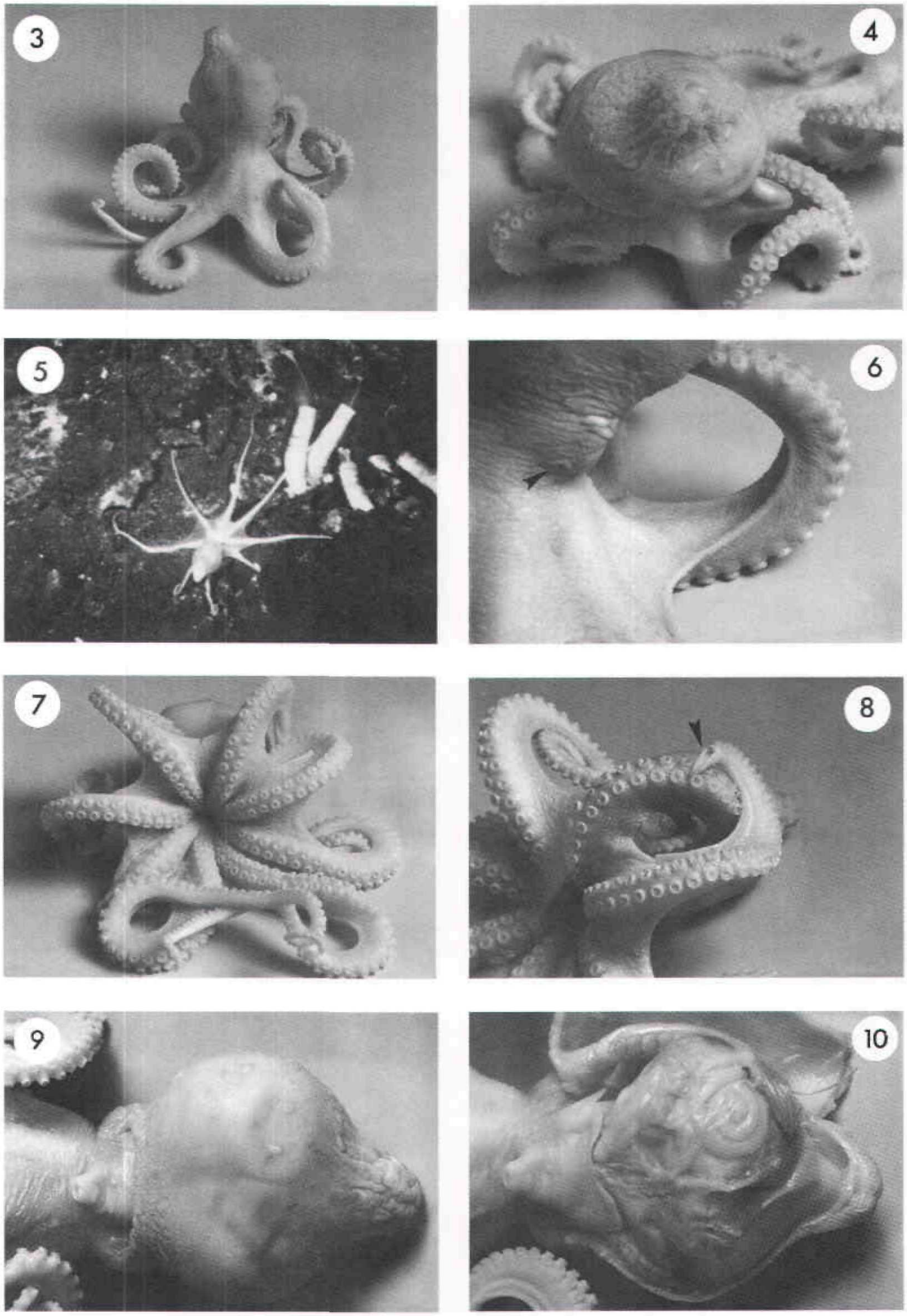

IV. Reproductive tract

The male reproductive system (Fig. 18) comprises a pear-shaped testis. Its posterior edge fits into the posterior part of the mantle. The vas deferens is relatively short and convoluted, its large, thick portion with many protuberances and secretory material (mucilaginous gland). Ampulla absent. Spermatophoric gland long and thick. Accessory gland small. Spermatophore storage sac (Needham's sac)

◀ **Figure 3.** Photograph of the holotype (dorsal view).
Figure 4. Photograph of the holotype (posterior view) showing the "mitre".
Figure 5. A specimen of *Vulcanoctopus hydrothermalis* photographed by the submersible *Cyana* (IFREMER / BIOCYARISE, D. Desbruyères, 1984) at the same site where the paratype was collected.
Figure 6. Position of the minute epidermal window *(arrow)* over the eye.
Figure 7. Oral view of arms and web.
Figure 8. Hectocotylized arm and ligula *(arrow)*.
Figure 9. Ventral view of the body and pallial aperture.
Figure 10. The mantle cavity opened to reveal the main features.

Figure 3. Photographie de l'holotype (vue dorsale).
Figure 4. Photographie de l'holotype (vue postérieure) montrant la "mitre".
Figure 5. Un spécimen de *Vulcanoctopus hydrothermalis* photographié par le submersible *Cyana* (IFREMER / BIOCYARISE, D. Desbruyères, 1984) à l'endroit où le paratype a été récolté.
Figure 6. Position de la petite fenêtre dans l'épiderme (flèche) sur l'œil.
Figure 7. Bras et membrane.
Figure 8. Bras hectocotyle et ligula *(flèche)*.
Figure 9. Vue ventrale du corps et fente palléale.
Figure 10. Cavité palléale ouverte montrant les organes en place.

very large, packed with 64 spermatophores in holotype. Spermatophores (Fig. 18C) are long (SpLI=125), white and golden in colour. Terminal organ (Fig. 18A) long with large diverticulum both being 47% of the ML.

Histological tranverse sections of the mucilaginous gland show that is composed by coiled tubules (Fig. 20). The lumen of that system is lined by a secretory epithelium and it is partially filled by sperm and a mucilaginous substance. The tubules are embedded in connective tissue.

V. Circulatory and excretory systems

The circulatory system is shown in Fig. 19. The position of the systemic heart is transversal. The main arteries that leave the ventricle (dorsal aorta, gonadal artery and abdominal artery) are illustrated in Fig. 19. The blood draining the head and the arms passes to the branchial hearts via the anterior vena cava and its two branches. The mesenteric sinus, which is separated in three regions, is well developed and it is connected to the vena cava via two large mesenteric or abdominal veins. These mesenteric veins join the vena cava before it is divided in two branches (lateral venae cavae). These pass through the renal sacs and open into the branchial hearts which send the blood to the gills. The blood returns via the auricles to the ventricle, then to arteries.

The veins are expanded into a series of diverticulae which protrude into the renal sacs, forming numerous lobules covered by the internal epithelium of the renal sacs. Histological sections of these renal appendages show them to consist of numerous venous diverticulae covered by a cubical epithelium and showing some muscles cells and nervous elements. Amoebocytes forming cellular clots can be observed in the mesenteric veins (Fig. 15), the distal part of the anterior vena cava, the lateral venae cavae and the venous diverticulae of the renal appendages (Fig. 14). The blood contains high concentrations of metals (Table 2).

VI. Eye

The eyes are covered by a thin semi-translucent skin of the head except a thinner semi-translucent skin forming a window of 0.2 mm long (Fig. 6). The eye is a simple closed cup with a lens. A large white body covers the eye, the optic nerves and the opic lobe (Fig. 26A, B). The optic nerves are long and end in the optic lobe. There is no trace of optic chiasma. The optic tract leaves the optic lobe to join the central nervous system through a small peduncle lobe.

A tranverse section of the eye is shown in Figs. 21 and 22. The back part of the eyeball is a pigmented retina (Fig. 21) and this is continuous with the ciliary muscle which supports the lens (Fig. 22). There is a cornea in the front of the eye ball and no trace of an iris (Fig. 22). The lens is peculiar with a plane surface between the ciliary muscles, then a constriction underneath this surface and the posterior part of the lens which is drop-like. The anterior part is difficult to distinguish in some sections, however there are three clear indications of its existence (Budelmann pers. comm.): a) the separation between the anterior and posterior parts runs exactly where the straight crack is, b) the colours of the anterior and posterior parts are different, and c) these two parts can be followed by their different colours up to the thinnest part which attach to the ciliary muscle (Fig. 22).

Histological section through the retina reveals four different layers from the centre of the eyeball to the periphery (Fig. 21) a) a thick layer with the distal segment of the visual cells; b) a thinner pigmented inner layer comprising the basal segments of the visual cells; c) a layer with the proximal segments of the visual cells and blood capillaries, and d) a plexiform layer. Underneath these

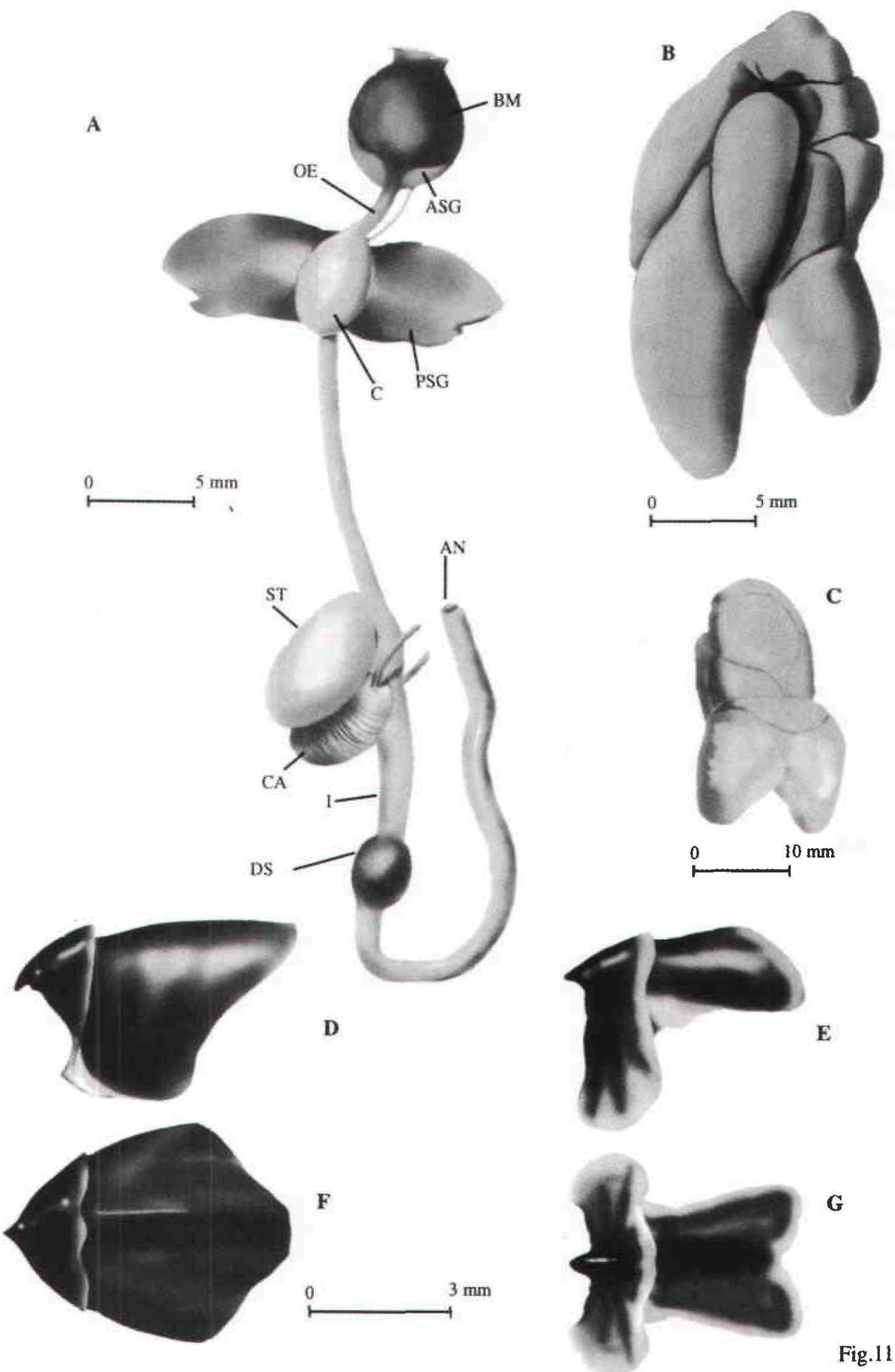

Figure 11. (**A**) The alimentary system. *(AN)* anus; *(ASG)* anterior salivary gland; *(BM)* buccal mass; *(C)* crop; *(CA)* caecum; *(DS)* dark swelling; *(I)* intestine; *(OE)* oesophagus; *(PSG)* posterior salivary gland; *(ST)* stomach. (**B**) Dorsal and (**C**) ventral view of the multilobulate digestive gland, with the anterior end at the top. (**D**) (**F**) Upper jaw. (**E**) (**G**) Lower jaw.

Figure 11. (**A**) Le système digestif. *(AN)* anus ; *(ASG)* glande salivaire antérieure ; *(BM)* masse buccale ; *(C)* jabot ; *(CA)* caecum; *(DS)* renflement noir ; *(I)* intestin ; *(OE)* œsophage ; *(PSG)* glande salivaire postérieure ; *(ST)* estomac ; vues dorsale (**B**) et ventrale (**C**) de la glande digestive multilobée, avec l'extrémité antérieure au sommet. (**D**) (**F**) mâchoire supérieure, (**E**) (**G**) mâchoire inférieure.

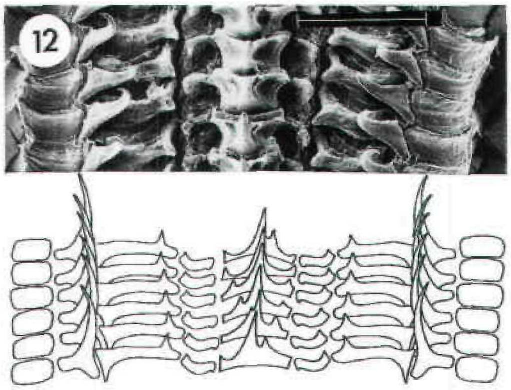

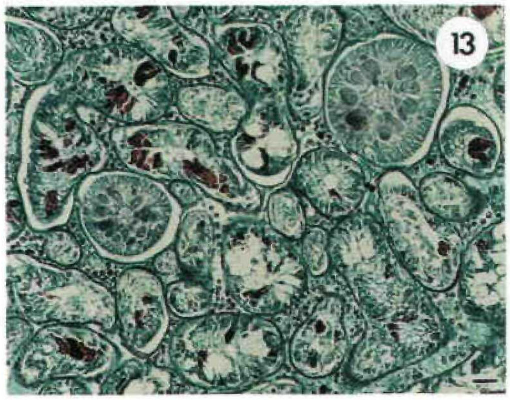

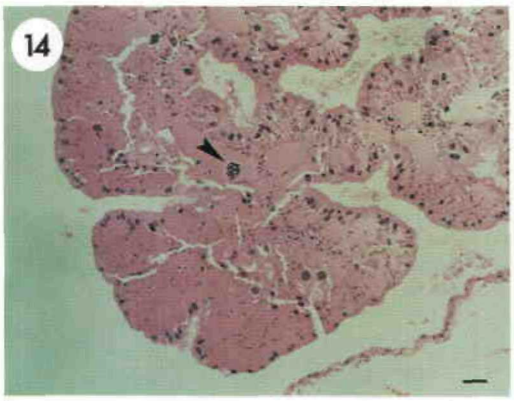

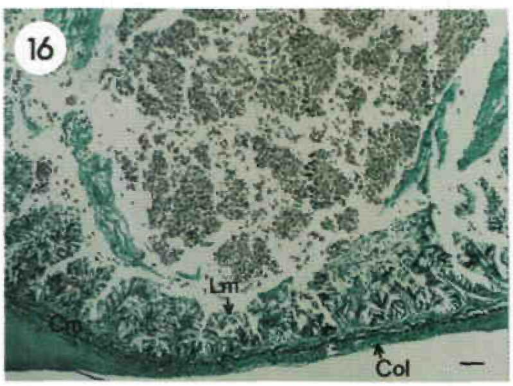

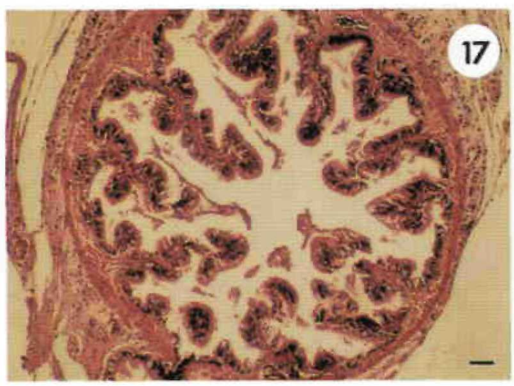

Figure 12. Scanning electron micrograph of the radula (top) and drawing of the teeth observed with the light microscope (below). Bar: 200 µm.

Figure 13. Transverse section of the posterior salivary gland. Bar: 50 µm.

Figure 14. Transverse section of the renal appendages showing an amoebocyte clot *(arrow)*. Bar: 125 µm.

Figure 15. Transverse section of a mesenteric vein with an amoebocyte clot *(arrow)*. Bar: 125 µm.

Figure 16. Transverse section of the dark swelling showing the substance that fills the lumen. *(Cm)* circular muscle; *(Col)* collagen; *(Lm)* longitudinal muscle. Bar: 125 µm.

Figure 17. Transverse section of the intestine below the dark swelling. Bar: 125 µm.

Figure 12. Micrographie au microscope électronique à balayage de la radula (en haut) et dessin des dents observées au microscope photonique (en bas). Échelle : 200 µm.

Figure 13. Coupe transversale de la glande salivaire postérieure. Échelle : 50 µm.

Figure 14. Coupe transversale des diverticules veineux de l'organe excréteur montrant un groupe d'amaebocytes *(flèche)*. Échelle : 125 µm.

Figure 15. Coupe transversale d'une veine mésentérique contenant un groupe d'amaebocytes (flèche). Échelle : 125 µm.

Figure 16. Coupe transversale du renflement noir montrant la substance qui remplit la lumière. *(Cm)* muscles circulaires ; *(Col)* collagène ; *(Lm)* muscles longitudinaux. Échelle : 125 µm.

Figure 17. Coupe transversale de l'intestin après le renflement noir. Échelle : 125 µm.

Table 2. Elemental concentrations (μg g^{-1} dry wt) in the venous system and mantle wall of *Vulcanoctopus hydrothermalis*.

Element	Abdominal vein	Lateral vena cava	Mantle wall
Al	6875	1320	954
Ba	124	39	55
Ca	343	281	875
Cd	35	17	13
Cu	1150	905	204
Fe	498	170	261
K	799	225	104
Li	0.498	0.17	0.065
Mg	1093	1426	2777
Mn	32	12	13
Ni	17	16	3.88
Pb	50	11	10
Sr	64	31	13
Zn	326	267	259

layers there is a layer of optic nerves which end in the optic lobe.

The skin covering the eye is composed (from outer to inner part, by 1) a layer of epithelial columnar cells, 2) a connective tissue, 3) a layer of longitudinal muscle fibres and 4) a layer of circular muscle fibres (Fig. 23). A transverse section of the white body is shown in Fig. 24. Mitotic activity and different stages of development of amoebocytes can be observed in the white body (Fig. 25).

VII. Stellate ganglia

The stellate ganglia (Fig. 26C) are located in the mantle wall, ventro-laterally. The pallial nerve reaches the body of the stellate ganglion in its middle part. The epistellar body is not included in the stellate ganglion. There are fifteen stellate nerves disposed radially and two broader stellate nerves that leave the stellate ganglion from a protuberance situated opposite to the epistellar body.

VIII. Metal analysis

The concentration of various elements (μg g^{-1} dry weight) in the abdominal vein, lateral vena cava and mantle wall are given in Table 2.

Discussion

A comparative evaluation of the familial characters in the Octopoda has been carried out. A muscular consistency of the body, suckers in two rows, umbrella short and mantle aperture not reduced are characters that place *Vulcanoctopus hydrothermalis* within the family Octopodidae (Nesis, 1987). However, there are several characters, some of which never described to date for incirrate octopods, that suggest the possibility of distinction a new sub-family of Octopodidae, the Vulcanoctopodinae. These characters are as follows: eye with no trace of iris, absence of optic chiasma, digestive gland multilobulate and presence of a dark swelling in the intestine. Nevertheless more material is needed for the erection of this new sub-family.

Vulcanoctopus hydrothermalis has characters that represent adaptations either to the deep-sea or to a hydrothermal vent habitat. The absence of ink sac, that has been considered as a primitive condition (Robson, 1932; Voss, 1988) has been explained by the adaptation of deep-water forms to a lightless habitat (Voss, 1988). Thus, up to the description of the shallow water octopod *Ameloctopus litoralis* Norman, 1992, the absence of ink sac was common to the Cirroctopoda and the Bathypolypodinae. The absence of ink sac appears to be related with the loss of the anal flaps (Norman, 1992), as observed in *V. hydrothermalis*.

V. hydrothermalis has a relatively large crop. A size reduction or loss of the crop is probably related, in other deep-sea octopods, to a diet of soft-bodied organisms (Voss, 1988). The diet of *V. hydrothermalis* does not appear to be related with this type of preys which is verified by the associated fauna and by the remains of integuments (probably belonging to galatheids) found in the stomach contents. Associated fauna and potential prey, *Alvinocaris lusca, Bythograea thermydron, Munidopsis subsquamosa* and *Bathymodiolus thermophilus*, were generally related to vestimentiferan tube worms *Riftia pachyptila*, in a zone of diffuse venting at temperatures ranging from 5°C to 30°C (Debruyères & Segonzac, 1997).

The caecum of *V. hydrothermalis* is a sac-like part of the digestive tract and is not coiled; this differs from the spiral caecum usually found in cephalopods (Mangold, 1989).

The dark swelling has a typical intestinal microstructure (see Budelmann et al., 1997). The submucosa is longitudinally folded with no secondary leaflets. The inner tall cylindrical epithelium contains secretory and ciliated cells. The lumen is filled with a secretion which may include heavy metals. The histology of the dark swelling appears also to be similar to an ink sac. During development the ink sac originates from an evagination of the 'intestinal anlage' and the ink is always discharged via the anus. The gland, in most cases has a long separate duct which, joins the rectum just before the anus. In our specimens, the dark swelling is an enlargement of both the intestinal walls and its lumen, in a short portion of the intestine. Thus, it is not an intestinal evagination, there is no ink duct, and the dark swelling excretes into the intestinal lumen. To understand the dark swelling as an ink sac, would imply the ink gland being embedded in the intestine walls and excreting in the intestinal lumen far from the anus. Presently this seems unsatisfactory.

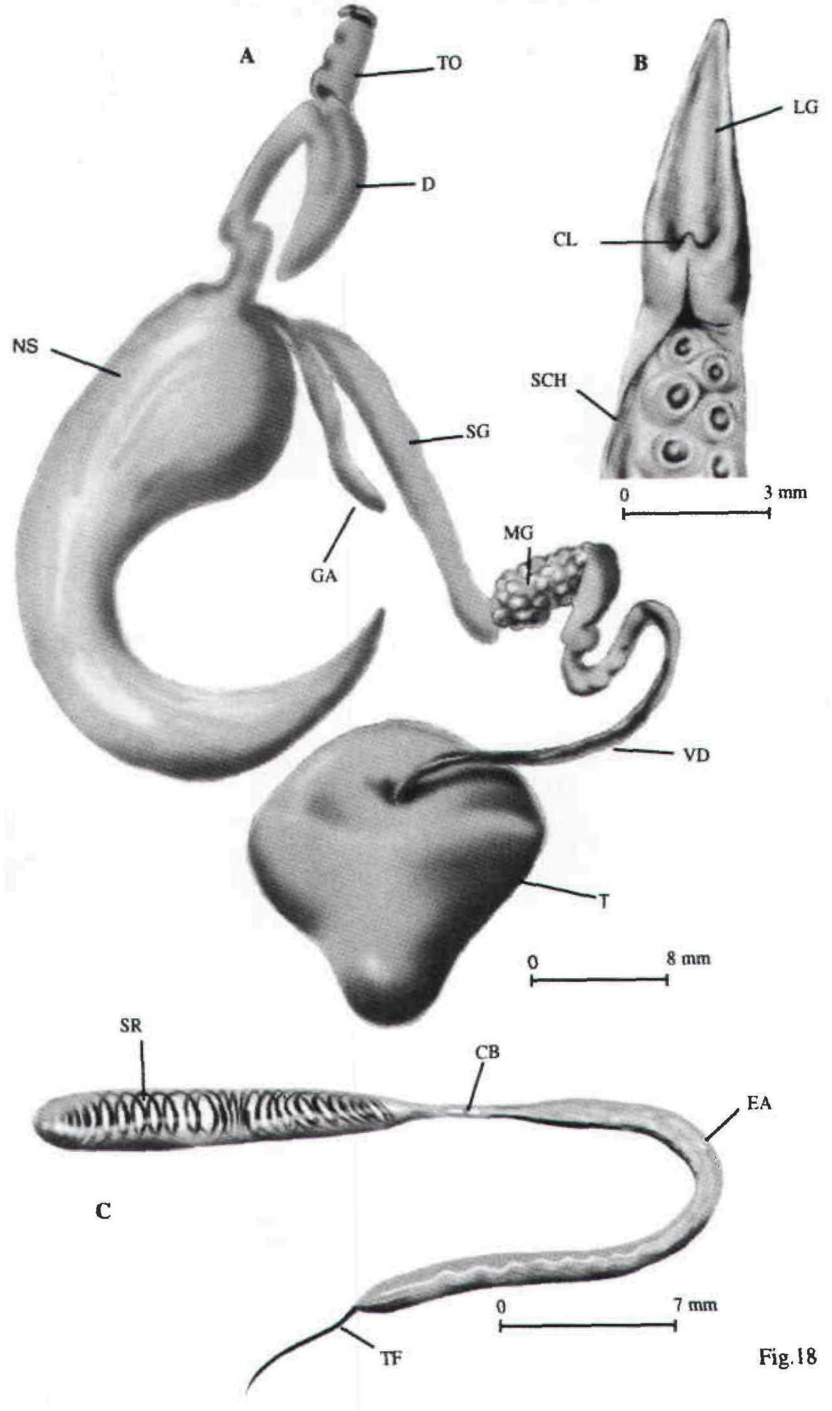

Figure 18. (**A**) Male reproductive system. *(D)* diverticulum; *(GA)* accessory gland; *(MG)* mucilaginous gland; *(NS)* Needham sac; *(SG)* spermatophoric gland; *(T)* testis; *(TO)* terminal organ; *(VD)* vas deferens. (**B**) Detail of the hectocotylus. *(CL)* calamus; *(LG)* ligula; *(SCH)* spermatophoric channel. (**C**) Spermatophore. *(CB)* cement body; *(EA)* ejaculatory apparatus; *(SR)* sperm reservoir; *(TF)* terminal filament.

Figure 18. (**A**) Appareil reproducteur mâle. *(D)* diverticulum ; *(GA)* glande accessoire ; *(MG)* glande mucilagineuse ; *(NS)* poche de Needham ; *(SG)* : glande spermatophorique ; *(T)* testicule ; *(TO)* organe terminal ; *(VD)* canal déférent. (**B**) Détail du bras hectocotyle. *(CL)* calamus ; *(LG)* ligula ; *(SCH)* canal spermatophorique (**C**) Spermatophore. *(CB)* glande cémentaire ; *(EA)* appareil éjaculatoire ; (SR) réservoir ; *(TF)* filament terminal.

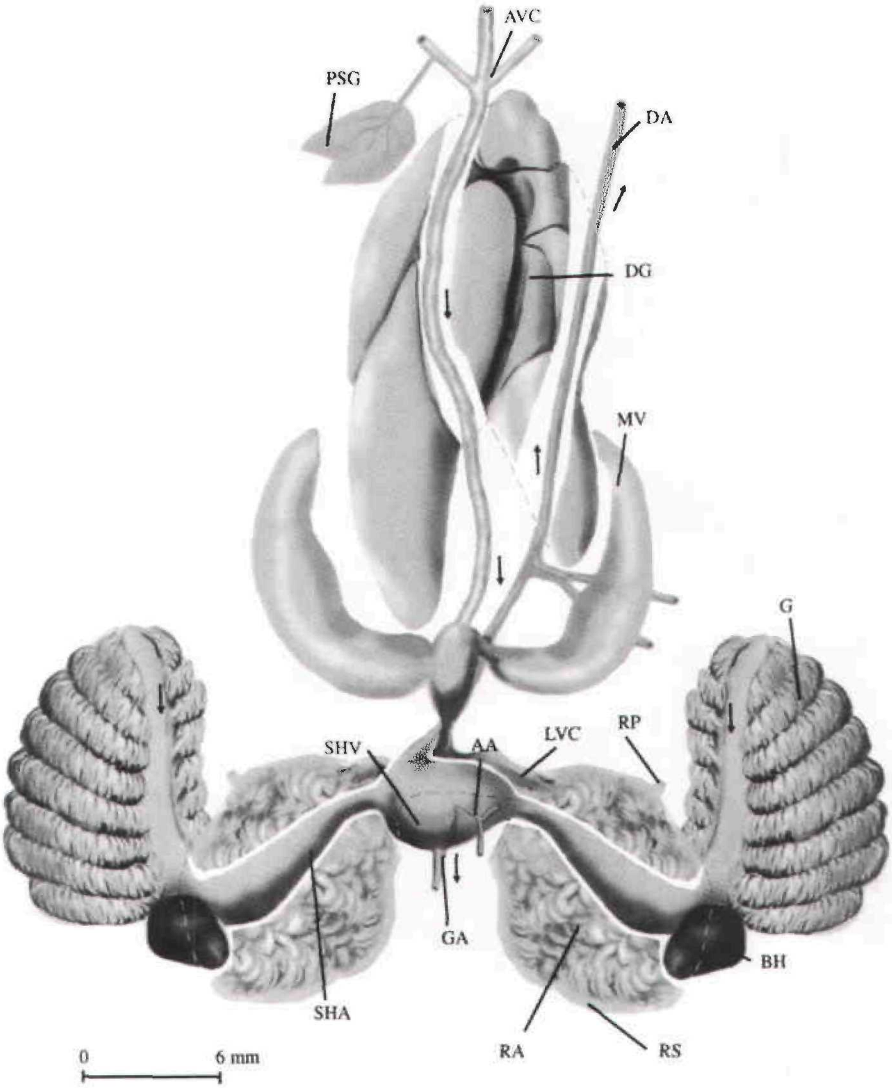

Figure 19. Circulatory and excretory systems. *(AA)* abdominal aorta; *(AVC)* anterior vena cava; *(BH)* branchial heart; *(DA)* dorsal aorta; *(DG)* digestive gland; *(G)* gill; *(GA)* gonadal artery; *(LVC)* lateral vena cava; *(MV)* mesenteric or abdominal vein; *(PSG)* posterior salivary gland; *(RA)* renal appendages; *(RP)* renal papilla; *(RS)* renal sac; *(SHA)* systemic heart auricle; *(SHV)* systemic heart ventricle.

Figure 19. Systèmes circulatoire et excréteur. *(AA)* aorte abdominale ; *(AVC)* veine cave antérieure ; *(BH)* cœur branchial ; *(DA)* aorte dorsale ; *(DG)* glande digestive ; *(G)* branchie ; *(GA)* artère génitale ; *(LVC)* veine cave latérale ; *(MV)* veine mésentérique ; *(PSG)* glande salivaire postérieure ; *(RA)* appendices rénaux ; *(RP)* papille rénale ; *(RS)* sac rénal ; *(SHA)* oreillette ; *(SHV)* ventricule.

The testis projects towards the posterior part of the mantle, giving the mantle a characteristic mitre-like shape. Video recording and pictures of alive specimens showed the same mitre-like posterior part of the mantle, indicating that this is not a fixation artefact (Fig. 5).

The visual system of this species lacks some of the features present in the eye of other cephalopods. All modern squid and octopuses examined so far, except *Cirrothauma,* have a vertical chiasma (Wells, 1978). However, the optic nerves of *V. hydrothermalis* project onto the optic lobe without inversion. This is also seen in the primitive lensless eye of *Nautilus* (Young, 1965) and the finned octopod *Cirrothauma,* the eye of which also lacks a lens (Aldred et al., 1983). Rather than a primitive state among coleoids, the absence of a chiasma is likely to be a secondary loss.

V. hydrothermalis inhabits an environment very close to the chimneys, where hydrothermal fluids are acidic, reduced and enriched with chemicals including heavy metals, methane, hydrogen sulphide and where there are also blooms of thermophilic bacteria (Prieur, 1997; Sarradin et

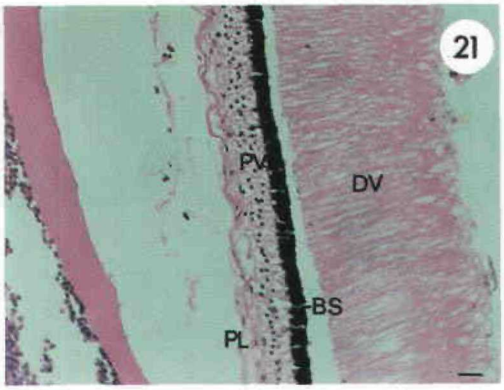

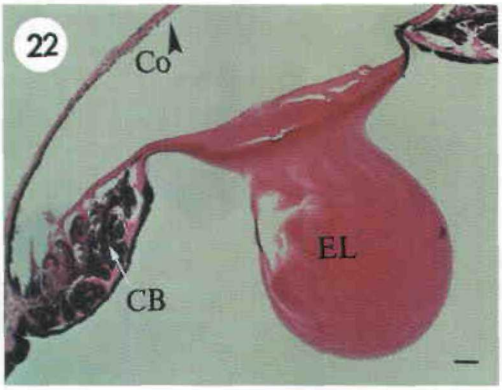

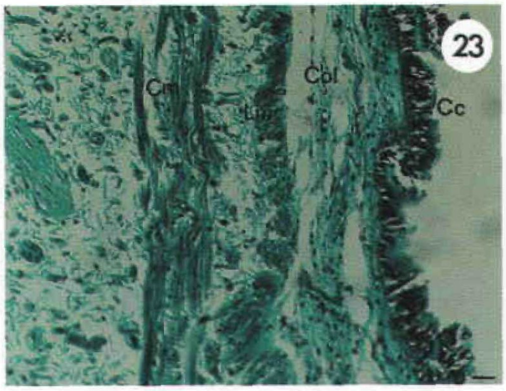

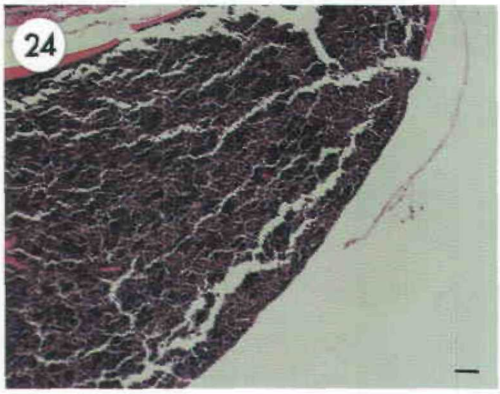

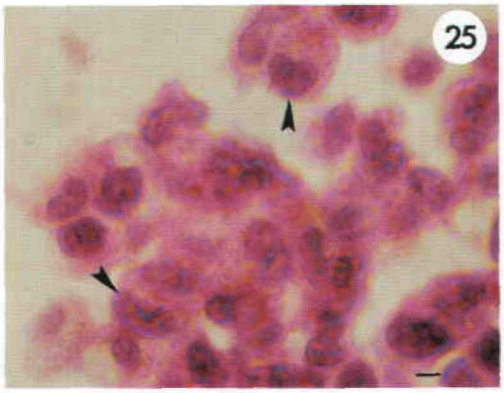

Figure 20. Transverse section of the mucilaginous gland of the male reproductive tract showing the tubules filled by sperm and mucilaginous secretion. Bar: 125 µm.

Figure 21. The rear part of the eye showing the layers of the retina. *(BS)* basal segments of the visual cells; *(DV)* distal segments of the visual cells; *(PL)* plexiform layer; *(PV)* proximal segments of the visual cells. Bar: 50 µm.

Figure 22. The front part of the eye. *(EL)* eye lens; *(Co)* cornea; *(CB)* ciliary body. Bar: 125 µm.

Figure 23. Transverse section of the skin of the head. *(Cc)* columnar cells; *(Cm)* circular muscle; *(Col)* collagen; *(Lm)* longitudinal muscle. Bar: 50 µm.

Figure 24. White body. Bar: 125 µm.

Figure 25. Hemopoietic cells of the white body and details of the mitotic activity *(arrow)*. Bar: 5 µm.

Figure 20. Coupe transversale de la glande mucilagineuse montrant la lumière de la glande remplie de sperme et d'une substance mucilagineuse. Échelle : 125 µm.

Figure 21. Partie profonde du globe oculaire montrant les couches de la rétine. *(BS)* segments basaux des cellules visuelles ; *(DV)* segments distaux des cellules visuelles ; *(PL)* couche plexiforme ; *(PV)* segments proximaux des cellules visuelles. Échelle : 50 µm.

Figure 22. Partie superficielle de l'œil. *(EL)* cristallin ; *(Co)* cornée ; *(CB)* corps ciliaire. Échelle : 125 µm.

Figure 23. Coupe transversale du tégument de la tête. *(Cc)* cellules columnaires ; *(Cm)* muscles circulaires ; *(Col)* collagène ; *(Lm)* muscles longitudinaux. Échelle : 50 µm.

Figure 24. Corps blanc. Échelle : 125 µm.

Figure 25. Cellules hématopoiétiques du corps blanc et détail de l'activité mitotique *(flèche)*. Échelle : 5 µm.

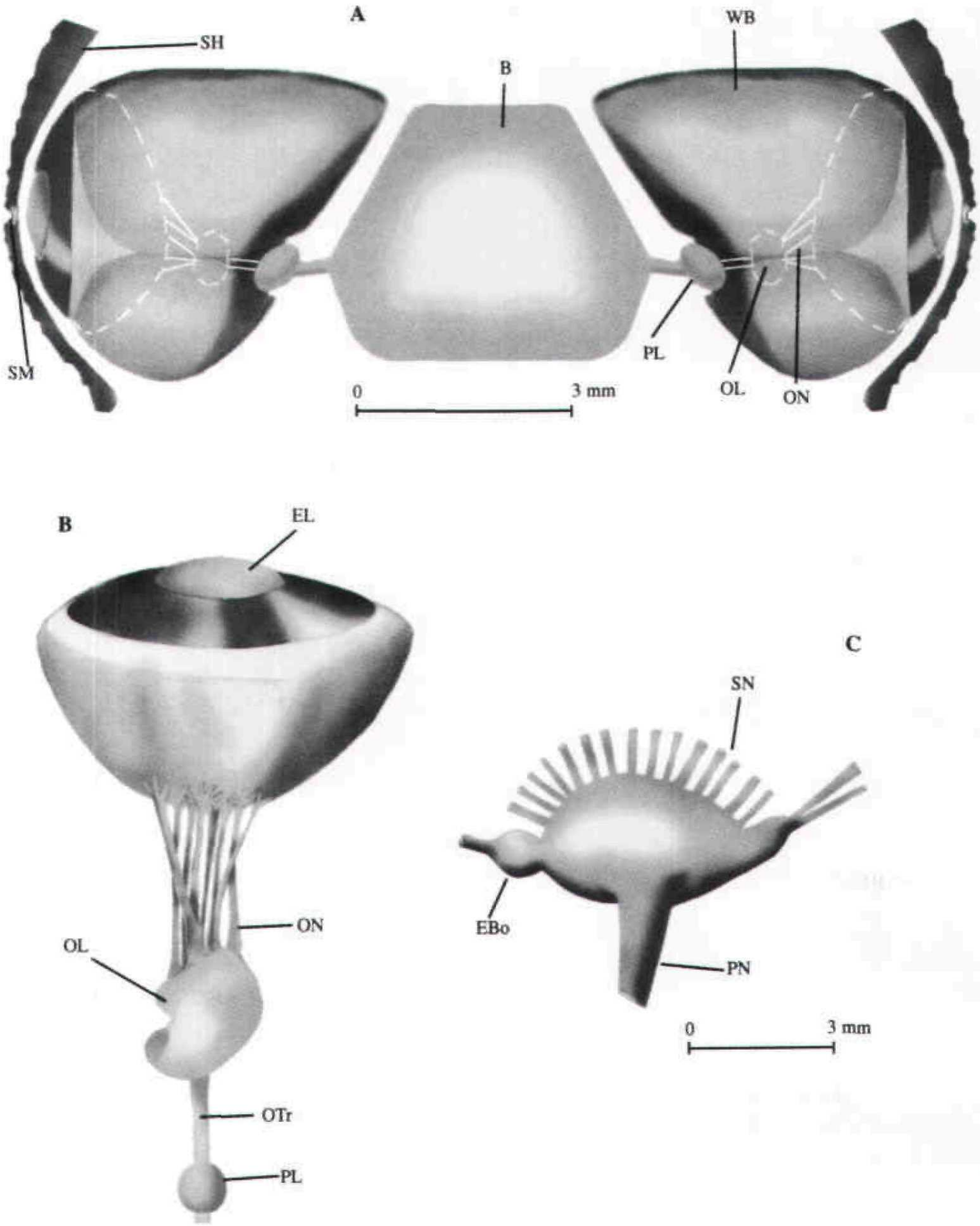

Figure 26. (A), (B): The visual system. *(B)* brain; *(EL)* eye lens; *(OL)* optic lobe; *(ON)* optic nerve; *(OTr)* optic tract; *(PL)* peduncle lobe; *(SH)* skin of the head; *(SM)* semi-translucent skin; *(WB)* white body. **(C)** Stellate ganglion. *(EBo)* epistellar body; *(PN)* pallial nerve; *(SN)* stellate nerve.

Figure 26. (A), (B) : Le système visuel. *(B)* cerveau ; *(EL)* cristallin ; *(OL)* lobe optique ; *(ON)* nerve optique ; *(OTr)* tractus optique ; *(PL)* lobe pedonculé ; *(SH)* épiderme de la tête ; *(SM)* membrane semi-transparente ; *(WB)* corps blanc. **(C)** Ganglion étoilé. *(EBo)* Corps épistellaire ; *(PN)* nerf palléal ; *(SN)* nerf étoilé.

al., unpublished). Amoebocytes clots are present in the blood of the venous system and concentrations of metals in the blood, as well as in the mantle wall, are much higher than those reported from oceanic squid, cuttlefish or other octopods (Sugiyama et al., 1989; Miramand & Bentley, 1992). These features appear as a response of this organism to the toxic hydrothermal environment they live in.

Cephalopods, like other molluscs have amoebocytes in their blood (diameter of 6-7 μm in *Octopus vulgaris*), with a lobulated nucleus filling much of the cell (Wells, 1978).

These wandering cells are part of a population that includes the large number of phagocytic cells found in the connective tissue and in the intercellular spaces of certain organs (Wells, 1978). Phagocytes have been found in the posterior salivary glands of *Eledone* when fine carbon particles are injected in the blood stream (Wells, 1978). It is well known that amoebocytes form cellular clots and are responsible for clearing foreign substances from the circulatory system (Ford, 1992). The size of these clots is remarkable in *V. hydrothermalis* sometimes being a hundred times bigger than a single amoebocyte. This is not surprising since the cells phagocytize bacteria that are probably present in high concentrations in the gut, gills and coelom of this animal. This clearing was observed in *Octopus dofleini* (Wülker, 1910), which phagocytize the bacterium *Serratia marcescens* Bizio, 1823, from the circulatory system within two hours of introduction (Bayne, 1973).

Vulcanoctopus hydrothermalis is the first octopod described to date in association with hydrothermal vents. This species offers a new insight on the adaptations that allow the colonization of this extreme environment by a cephalopod. Further studies of the octopod fauna associated to hydrothermal vents, that can be considered as ephemeral biogeographical islands to their endemic faunas (see Gage & Tyler, 1997) and that have shown different stages of evolution after catastrophic events (Briand et al., 1997), will increase our knowledge on the evolution of these cosmopolitan mollusks in this special environment.

Acknowledgements

This work was funded by the URM 7 IFREMER and DORSALES Program. We wish to express our appreciation to Dr. Françoise Gaill (CNRS, Paris), Chief Scientist on the HOT 96 Cruise, for the facilities provided, and to all the participants of the cruise for their cooperation. We thank the anonymous referees of this paper whom comments largely improved the manuscript. We also thank Drs. M. Nixon, L. Allcock, U. Budelmann, M. Norman, C. Jouin-Toulmond, A. Toulmond and Mr. M. Segonzac for their helpful criticism and corrections on different drafts of the manuscript, C.A.C.T.I. (University of Vigo, Spain) for the analysis of elements and Mr. A. López "Tokio" for the drawings.

References

Aldred R.G., Nixon M. & Young J.Z. 1983. *Cirrothauma murrayi* Chun, a finned octopod. *Philosophical Transactions of the Royal Society of London* B, **301**: 1-54.

Bayne C.J. 1973. Internal defense mechanism of *Octopus dofleini*. *Malacological Review,* **6**: 13-17.

Briand P., Desbruyères D., Jollivet D., Alayse A.M., Childress, J.J., Gaill F. & Lutz R. 1997. Pluriannual temporal change in vent communities at Genesis Parigo-Pogosud vent sites (East Pacific Rise, 12°48'N & 103°56'W). First International Symposium on deep-sea hydrothermal vent biology. Funchal, Madeira (Abstr.).

Budelmann B.U., Schipp R. & Boletzky S.v. 1997. Cephalopoda. In: *Microscopic anatomy of invertebrates.* Vol 6, Mollusca II (F.W. Harrison & A.J. Kohn eds.) pp. 119-414. New York: Wiley-Liss.

Campbell A.C., Palmer M.R., Klinkhammer G.P., Bowers T.S., Edmond J.M., Lawrence J.R., Casey J.F., Thompson G., Humphris S., Rona P. & Karson J. 1988. Chemistry of hot springs on the Mid-Atlantic Ridge. *Nature,* **335**: 514-519.

Chevaldonné P. 1997. The fauna of deep-sea hydrothermal vent: an introduction. In: *Handbook of deep-sea hydrothernal vent fauna.* (D. Desbruyères & M. Segonzac, eds.). Editions IFREMER, Brest: 7-10.

Clarke, M.R. 1986. *A handbook for identification of cephalopod beaks.* Clarendon Press, Oxford. 273 pp.

Clarke M.R. & Trueman E.R. 1988. Introduction. In: *The Mollusca.* Vol 12. *Paleontology and Neontology of Cephalopods* (M.R. Clarke & E.R. Trueman, eds.), pp. 1-10. London, Academic Press Inc.

Desbruyères D. & Segonzac M. (eds.) 1997. The fauna of deep-sea hydrothermal vent: an introduction. Editions IFREMER, Brest, 279 pp.

Desbruyères D., Crassous F., Grassle J., Khripounoff A., Reyss D., Rio M. & Van Praet M. 1982. Données écologiques sur un nouveau site d'hydrothermalisme actif de la ride du Pacifique oriental. *Comptes Rendus de l'Académie des Sciences de Paris,* **295**, Série III: 489-494.

Ford L.A., 1992. Host defense mechanisms in cephalopods. *Annual Review of Fish Diseases,* 25-41.

Fustec A. 1985. Microdistribution et variations temporelles de la faune hydrothermale des sites de la zone "13°N" sur la ride du Pacifique Est. PhD Thèse, University of Rennes, 146 pp.

Gage J.T. & Tyler P.A. 1991. Deep-sea hydrothermal vents and cold seeps. In: *Deep-sea biology. A Natural history of organisms at the deep-sea floor.* (J.T. Gage & P.A . Tyler, eds.), pp. 363-391. Cambridge: University Press.

Guerra A., Villanueva R., Nesis K.N. & Bedoya J. In press. Redescription of the deep-sea cirrate octopod *Cirroteuthis magna* Hoyle, 1885 and considerations on the genus *Cirroteuthis* (Mollusca: Cephalopoda). *Bulletin of Marine Science.*

Leach W.E. 1817. Synopsis of the Orders, Families and Genera of the Class Cephalopoda. *Zoological Miscellany,* **3**: 137-141.

Londsdale P. 1977. Clustering of suspension feeding macrobenthos near abyssal hydrothermal vents at oceanic spreading centers. *Deep-Sea Research,* **24**: 857-863.

Lutz R.A. & Voight J.R. 1994. Close encounter in the deep. *Nature,* **371**: 563.

Lutz R.A. & Voight J.R. 1997. *Graneledone* spp. and *Benthoctopus* spp. In: *Handbook of deep-sea hydrothernal vent fauna.* (Desbruyères D. and Segonzac M., eds.). Editions IFREMER, Brest, 158-159.

Mangold, K. (ed.) 1989. Céphalopodes. V(4). In: *Traité de Zoologie*. (P.P. Grassé, ed.). Masson, Paris, 804 pp.

Miramand P. & Bentley D. 1992. Concentration and distribution of heavy metals in tissues of two cephalopods, *Eledone cirrhosa* and *Sepia officinalis,* from the French coast of the English Channel. *Marine Biology,* **114**: 407-414.

Nesis K.N. 1987. *Cephalopods of the world.* TFH Publications, Neptune City: New Jersey. 351 pp.

Norman M.D. 1992. *Ameloctopus litoralis*, gen. et sp. nov. (Cephalopoda: Octopodidae), a new shallow-water octopus from tropical Australian waters. *Invertebrate Taxonomy,* **6**: 567-582.

Prieur, D. 1997. Microbiology of deep-sea hydrothermal vents. *TIBTECH,* **15**: 142-244.

Robson G.C. 1932. A monograph of a recent Cephalopoda. In: Part II. *The Octopoda* (excluding the Octopodinae). London: British Museum (Natural History), 359 pp.

Roper C.F.E. & Voss G.L. 1983. Guidelines for taxonomic descriptions of cephalopod species. *Memoirs of the National Museum of Victoria,* **44**: 49-63.

Sarradin P.M., Caprais J.C., Briand P., Gaill F., Shillito B. & Desbruyères D. 1998. Chemical and thermal description of the *Genesis* hydrothermal vent community environment (13°N, EPR). *Cahiers de Biologie Marine.,* **39**: 159-167.

Sugiyama M., Kousu S., Hanabe M. & Okuda Y. 1989. Chemical properties. In: *Utilization of squid,* pp. 59-111. Amsterdam: A. A. Balkema.

Villanueva R., Segonzac M. & Guerra A. 1997. Locomotion modes of deep-sea cirrate octopods (Cephalopoda) based on observations from video recordings on the Mid-Atlantic Ridge. *Marine Biology,* **129**: 113-122.

Voss G.L. 1988. Evolution and phylogenetic relationship of deep-sea octopods (Cirrata and Incirrata). In: *The Mollusca. Vol 12. Paleontology and Neontology of Cephalopods* (M.R. Clarke & E.R . Trueman, eds.), pp. 253-276. London: Academic Press.

Wells M.J. 1978. *Octopus: Physiology and Behaviour of an Advance Invertebrate.* London: Chapman & Hall, 417 pp.

Young J.Z. 1965. The central nervous system of *Nautilus. Philosophical Transactions of the Royal Society of London* B, **249**: 1-25.